TAILORING THE BENDING STIFFNESS OF ELASTOMERIC DUAL-MATRIX LAMINATES

Platt, D.[1]*, Steeves, C.[2]
[1] UTIAS, University of Toronto, Toronto, Canada
[2] UTIAS, University of Toronto, Toronto, Canada
* Corresponding author (d.platt@mail.utoronto.ca)

Keywords*: aerospace, dual-matrix composites, morphing.*

ABSTRACT

The increasing environmental impact of aviation has led to mounting pressure on aircraft companies to develop innovative technologies for sustainable aviation. One area of development is aircraft structural design, which is becoming increasingly oriented towards multifunctional structures that can withstand large loads while exhibiting additional functional capabilities; morphing is an example. Composite materials provide an ideal platform for the advancement of such morphing technologies, due to the superior design flexibility with respect to the numerous input parameters. This work investigates dual-matrix composites (continuous fibres embedded in distinct epoxy and elastomer matrix regions) for structural applications in aircraft; the technology is being investigated by several researchers, but its feasibility in high-load applications is yet to be explored. The macromechanics of dual-matrix laminates are investigated, with the focus being the tailoring of the bending stiffness of such laminates. The stiffness of a dual-matrix hinge can be tailored in a few ways. The primary variables are the thickness, width, length, and layup orientation; the primary focus of this work is the width and thickness of the laminates. These specific parameters play an important role in the anticlastic bending behavior of the laminates. Significant cross-section anticlastic deflections of $[\pm 45_n]$ layups, due to high Poisson ratios close to unity, are shown to increase the bending stiffness of the laminate, resulting from an increased second moment of area. A predictive model for the increase in bending stiffness is constructed and compared with Abaqus FEA and experiments. Challenges associated with this model include the interaction effects between the rigid and compliant regions, and the modelling of woven-fabric composites using Classical Lamination Theory (CLT), which proves inadequate due to large deformations and unique inter- and intra-lamina shear behaviour.

1 INTRODUCTION

Global aviation, like other forms of transport, is under increasing pressure to become sustainable. Typically, the primary focus is on engine efficiency but many other factors also influence the efficiency of an aircraft, one of which is the structural weight. There are several ways to reduce the structural weight of an aircraft, with the most prevalent design method being the use of alternative materials, specifically fibre composites, which exhibit superior strength- and stiffness-to-weight properties. Many new aircraft designs make extensive use of composites, specific examples of this being the Boeing 787 and Airbus A350. Composites have superior design flexibility compared to most materials, allowing for stiffness tailoring.

A combination of the transition to composite materials and the desire for morphing has resulted in recent research into morphing composites. The desired benefit of morphing is a multi-functional structure which achieves large deformations without compromising its load-carrying capability. There are various methods that are investigated by other researchers (a more detailed review can be found in [1]), but this work particularly

investigates dual-matrix composite structures, and certain phenomena associated with the bending of such composites.

1.1 Stiffness Tailoring of Composites

The most challenging design requirement of a morphing structure is a skin that exhibits both in-plane compliance and out-of-plane stiffness. There has been significant research in the development of skins suitable for morphing applications as reviewed by Thill *et al.* [2]. An example of morphing would be a variable aspect ratio wing, where the area change of the skin requires it to be stretched. Typical aerospace materials such as aluminum are extremely resistant to stretching or sheering and are therefore unsuitable.

Elastomers, such as silicone rubber, are capable of large elastic strains (more than 400%) but they are not ideal for load carrying due to their high compliance. In a related material, flexible matrix composites (FMCs), fibres provide the required strength while an elastomeric matrix provides increased strain capability. For example, Murray *et al.* [3] propose a one-dimensional morphing laminate wherein the stiffness of the elastomeric composite laminate is tailored by orienting the fibres predominantly in the desired morphing direction, to maximize the difference in perpendicular elastic moduli. However, this has some limitations with low out-of-plane stiffness

A traditional fibre-epoxy laminate can be combined with the FMC, resulting in what is known as a dual-matrix composite, where multiple matrix materials with different properties are used in discrete regions to tailor the local stiffness. Dual-matrix composites are arguably the most practical for morphing applications, given their compactness, low weight, relative ease of manufacture, and superior stiffness tailoring capability. Jiménez [4] presents a folding design of a silicone/epoxy dual-matrix composite. The panels of the structure are epoxy-reinforced glass fibres, while the folds have a silicone-based matrix. The elastomeric silicone permits large curvature changes with folds close to 180° being demonstrated. This laminate is fabricated using UV-cure silicone but this processing path can be limiting, since it requires translucent fibres, such as glass, while many applications require opaque Kevlar or carbon fibre. Section 2.2 describes the manufacturing process used in this work using carbon fibre and a two-part curing elastomer.

1.2 Anticlastic Effects in Laminated Composite Beams

The bending of a plate or beam is typically accompanied by an anticlastic curvature in the orthogonal direction to the axis of applied curvature as shown in Figure 1. The deformed shape of the cross section due to the anticlastic effect has been investigated thoroughly with some of the first work being conducted by Ashwell [5], who models this behaviour in isotropic plates. Pomeroy [6] expands on the previous work of Ashwell by investigating the impact of this phenomenon on a beam's cross-sectional second moment of area. This work provides valuable insight into the transition between narrow beam theory and wide beam theory. When a principal curvature, κ_x, is induced in a narrow beam by an applied moment, *M*, the transverse anticlastic

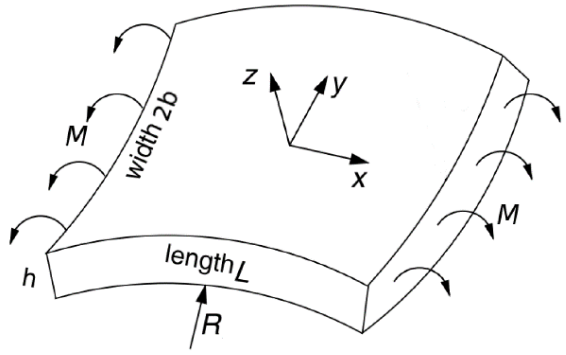

Figure 1. Anticlastic effect in a beam due to an applied moment (Modified from original source [7])

curvature, κ_y, is defined by

$$\kappa_y = -\nu\kappa_x, \tag{1}$$

where ν is the Poisson ratio. Thus, the transverse curvature is a linear function of the principal curvature. In wider beams however, these curvatures have a non-linear relationship. Pomeroy uses the assumption that the anticlastic curvature can be represented by a beam on an elastic foundation to derive an expression for the curvature of a wide beam and shows that the curvature near the edges of the cross-section follows the narrow beam theory whilst the curvature elsewhere is the second derivative of the anticlastic deflection, which is defined later. This work is useful for understanding the transition from narrow beam to wide beam behavior, but specifically applies to isotropic materials with $\nu \leq 0.5$. Composites, however, can exhibit larger Poisson ratios, particularly [±45] laminates. Pao [8], and Hyer and Bhavani [9], extend the theory to composite laminated plates. The authors derive theoretical models to predict the deformed shape of the plate cross-section for an induced longitudinal radius of curvature, *R*. This theoretical model forms the foundation of this work and is presented in detail in Section 3.

2 FABRICATION PROCESS AND MATERIAL CHARACTERIZATION

2.1 Material Selection

Freeman Manufacturing 3K tow plain-weave carbon fibre fabric (with a weight of 5.7 oz./sq.yd.) is used in this work because of its superior workability compared to other weaves and unidirectional fabric. Furthermore, plain-weave fabric is advantageous over other weave patterns, since the fibre tow length for each undulation of the weave is as small as possible, which has greater resistance to fibre-tow buckling [10].

Two matrix materials with significantly different elastic moduli are essential to ensure that there is a large enough disparity in the bending stiffness of each region of the laminate. Epoxy resin (Araldite LY 8601 / Aradur 8602 System) is used in the rigid section and polyurethane elastomer (Freeman 1040) is used for the compliant section. The latter is chosen by comparing several elastomers including silicone-based materials. Freeman 1040 is chosen due to its high compliance, relatively low cost and its rapid gel time of 28 minutes, which is advantageous for isolating the elastomeric resin, preventing excessive seepage of the resin outside the intended area of application when curing.

2.2 Dual-Matrix Fabrication

A two-stage fabrication process is employed for the manufacture of the dual-matrix laminate. The first stage involves the full curing of the isolated elastomeric regions of the laminate, while the second stage entails the application of epoxy resin to the remaining regions (the cured elastomer region acts as an impervious barrier, prohibiting overlapping of resins). In the first stage, the elastomeric resin does not spread much beyond its initially defined boundaries, due to the low gel time, which is desirable. Visuals of the process and a detailed step-by-step procedure can be found in [1]. The biggest challenge in this procedure is to avoid the formation of voids when the process is lengthy (for a laminate of many layers, for example).

2.3 Composite Mechanical Properties

All tensile and compressive testing is conducted using a MTS 880 Material Test System with a 100 kN load cell. An Electronic Instrument Research LE-05 laser extensometer is used for strain measurements. The tensile specimens are gripped using mechanical grips while the compression specimens are fixed in a Wyoming Test Fixtures Inc. compression test fixture to ensure accurate alignment. The material properties obtained through testing are summarized in Table 1.

Table 1. Measured material properties

Parameter	Elastomer	CF/epoxy [(0/90F[1])]	CF/epoxy [±45F]	CF/elastomer [(0/90F)]	CF/elastomer [±45F]
E_t (MPa)	2.47	45,300	11,900	21,000	38.0/117[2]
E_c (MPa)	-	73,500	7,920	-	-
ν_{xy}	0.45-0.5	0.09	0.85	0.55	~1.0

[1] 'F' denotes a plain weave fabric
[2] See following explanation

The [±45F] elastomeric laminate exhibits interesting tensile properties with the stress-strain relationship being bilinear. The elastic modulus is measured as initially 117 MPa, and transitioning to 38.0 MPa for increasing strain. This is important to note when considering the bending behavior of a laminate which encounters stresses and strains in this transition region (not relevant in the experiments in this work).

3 ANTICLASTIC BENDING

The theoretical model for anticlastic effects in composite laminates derived by Hyer and Bhavani is well defined and presented here. However, the increase in bending stiffness in composite laminates due to anticlastic bending is yet to be characterized accurately, to the best knowledge of the authors of this work. The anticlastic effect has a significant impact on the effective bending stiffness of a dual-matrix laminate, which is further discussed in this section.

3.1 Anticlastic Bending Governing Equation

The deflection in the *z*-direction, *w*, of the plate's cross-section for a given longitudinal radius of curvature is governed by the fourth-order ordinary differential equation (ODE)

$$\frac{\mathrm{d}^4 W}{\mathrm{d}Y^4} + 4\beta^4 w(y) = 0, \tag{2}$$

where $W = w/h$, $Y = y/b$, h is the thickness of the plate, $2b$ is the width of the plate, $\beta^4 = 3(1-\nu^2)/(R_x^2 h^2)$, and R_x is the longitudinal radius of curvature. For application to composite analysis, a modified form of this ODE is presented by Hyer and Bhavani using an inverted form of the laminate load-strain relationship, given by

$$\begin{Bmatrix} \varepsilon \\ M \end{Bmatrix} = \begin{bmatrix} A^* & B^* \\ -(B^*)^T & D^* \end{bmatrix} \begin{Bmatrix} N \\ \kappa \end{Bmatrix}, \tag{3}$$

where $A^* = A^{-1}$, $B^* = A^{-1}B$, and $D^* = D - BA^{-1}B$. Using the same approach, Pao presents the modified governing equation for a composite plate as

$$\frac{\mathrm{d}^4 W}{\mathrm{d}Y^4} - \left[\frac{2B_{21}^*\lambda}{A_{22}^* D_{11}^* + {B_{21}^*}^2}\right]\frac{\mathrm{d}^2 W}{\mathrm{d}Y^2} + \frac{(h\lambda)^2}{A_{22}^* D_{11}^* + {B_{21}^*}^2} W = 0, \tag{4}$$

where, $\lambda = b^2/(R_x h)$. The general solution of this ODE is

$$W = C_1 \sinh \alpha Y \sin \alpha Y + C_2 \cosh \alpha Y \cos \alpha Y, \tag{5}$$

where $\alpha = [b^4/(A_{22}^* D_{11} R_x^2)]^{1/4}$ (obtained from [9]) and the two integration constants, C_1 and C_2 are obtained by imposing the appropriate boundary conditions, namely that the internal bending moment and shear force at the edges of the plate ($Y = \pm 1$) are zero.

3.2 Finite Element Model Limitations

The Abaqus/Standard finite element model in this work is a three-dimensional (3D) shell analysis. Since this work considers pure bending in thin laminates, four-noded reduced integration shell elements are chosen, which also allow for simple management of the laminate cross-section properties and minimize the computational cost. The model used in this analysis has certain limitations that affect the simulation accuracy, primarily the section definition of the composite layup. Woven-fabric composites are the most commonly used for wet layup, yet Abaqus does not provide an option for modelling woven-fabric composites; instead, the laminae are all unidirectional. The simplest approximation to the woven-fabric laminates used in this work is to specify a symmetric unidirectional layup of alternating orientations, e.g. $[(\pm 45)_2]_S$. However, the behaviour of laminates of this orientation is highly dominated by shear, for which there is expected to be a significant difference between woven-fabric and unidirectional laminae. The FEA shows that the shear strain, LE_{12}, is dominant by three orders of magnitude compared to the normal strain, LE_{11}. It can be seen that the magnitude of the shear strain across subsequent laminae is continuous, but of opposite sign. This shear strain distribution is expected to look significantly different for a woven-fabric laminate, since there is interaction between the interwoven fibre tows of perpendicular orientation.

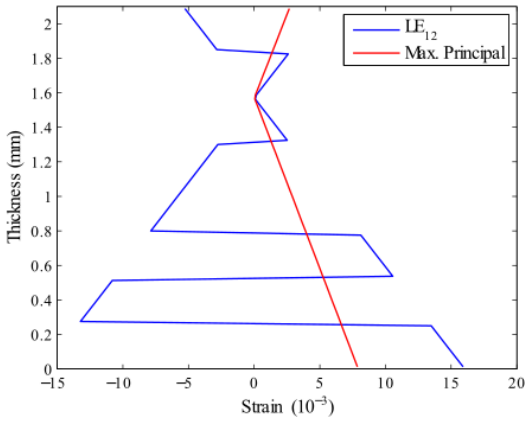

Figure 2. Abaqus output for through-thickness logarithmic strains of a $[(\pm 45)_2]_S$ elastomeric laminate

Several authors have modelled the properties of woven fabrics, although most of the research has been conducted at the unit cell level by modelling repeating unit cells of overlapping fibre tows. The overall behaviour of the laminate is of interest here, so detailed modelling at this level becomes intensive. The only alternative is to modify the stiffness matrices in Abaqus. Raju and Wang [11] present modified CLT models for various weave patterns. These models can be used in the FEM for better predictions of the behaviour of woven composites. This is outside the scope of this work and is recommended for further development.

3.3 Increase in Bending Stiffness Due to Anticlastic Effects

In order to simplify the analysis, the laminate is approximated as a homogeneous material with constant elastic modulus and a large Poisson ratio, close to unity. Therefore, the bending stiffness, *EI*, of the laminate can be approximated using the elementary beam theory equation,

$$EI = \frac{M}{\kappa}, \tag{6}$$

where M is the internal bending moment, and κ is the curvature of the beam; for pure bending of a beam with uniform cross section, κ is constant. Obtaining these values experimentally or through FEM allows for the bending stiffness to be determined and compared with theoretical predictions. Naturally, with a deformed cross section (due to anticlastic effects), bending of thin laminates results in an increased second moment of area, I. The second moment of area is calculated by discretizing the cross-section and integrating along the width. Assuming the elastic modulus to be constant (although not always true), the bending stiffness increases due to anticlastic curvature.

3.3.1 Neutral Axis Shift

The geometric neutral axis of a cross section may not necessarily be the actual neutral axis when a beam or plate is subjected to a bending moment. It is well documented in the literature that the neutral axis does not coincide with the centroid for curved beams. This also applies to beams subject to large curvatures, where the small deflection assumption is no longer valid. In a curved beam, the neutral axis is normally shifted toward the concave side of the beam, however the neutral axis in this case moves toward the convex side due to the anticlastic effect. This is most prominent in wider laminates, which may be a consequence of transition to wide-beam anticlastic behavior. Most composite applications employ thin laminates, so the anticlastic effect has a greater impact on the location of the neutral axis and thus, the second moment of area. The combination of small thickness and relatively large shift in neutral axis compounds the increase in the second moment of area of the laminate. It is found that the neutral axis location is a linear function of the longitudinal curvature of the laminate. There exists a discrepancy between FE and theory which, to the best knowledge of the authors, has not previously been characterized. This discrepancy in the neutral axis location increases with increasing curvature. The most likely explanation for this is that the wide beam theory influences the neutral axis location. In the FE analysis, the maximum principal strain, overlaid in Figure 2 (shear strain), reveals the point of zero principal strain, indicating the location of the neutral axis of the cross-section.

3.3.2 Bending Stiffness

The analytical model demonstrates a close correlation with the FEA. However, as the curvature increases, the predicted bending stiffness of the FE model increases at a greater rate than for the analytical model, as seen in Figure 3. This is likely due to the transition from narrow- to wide-beam theory of the anticlastic effect; additional strain energy is stored due to the anticlastic curvature being constrained (this is demonstrated clearly in Section 4.1). Conversely, it is found that the model slightly overpredicts the bending stiffness for narrow laminates. The trend lines in Figure 3 are intended to demonstrate the non-linearity of the bending stiffness. Based on the analytical model, the increase in bending stiffness is greater for thinner laminates than for thicker laminates, for the same width and curvature. For example, the bending stiffness of a 40 mm wide, 1 mm thick laminate increases by a factor of five for κ_x=10 m^{-1}, while only a factor of two for the 2 mm thick laminate. This is due to the thicker laminate exhibiting smaller anticlastic deflections, in addition to its eightfold greater zero-curvature bending stiffness, $(EI)_0$. The increase in bending stiffness is larger for wider laminates, which is to be expected as the deflections are larger compared to narrower laminates. However, for very wide laminates (>60 mm) exposed to large curvatures, the bending stiffness begins to plateau. This is due to the wide-beam theory coming into effect, whereby the central region of the laminate flattens as the curvature increases. Such excessive curvatures are impractical as the laminate is damaged by fibre-tow buckling well before these curvatures are obtained. Other laminate layups have a smaller increase in bending stiffness since the anticlastic effect is maximized with the [±45] layup. $(EI)_0$ increases rapidly as the orientation approaches 0°, so the morphing capability is significantly impaired. Conversely, if the layup approaches 90°, $(EI)_0$ becomes extremely

small and the laminate is too flexible. The characterization of this bending stiffness increase provides a simple yet relatively accurate method for predicting the bending behaviour of elastomeric composites.

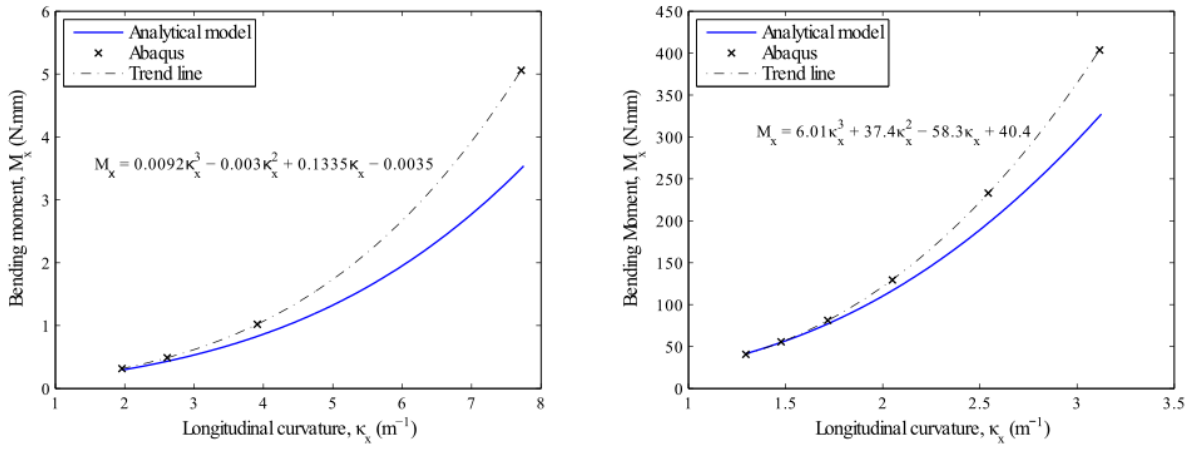

Figure 3. Applied bending moment required for increasing longitudinal curvature of (a) 40 mm wide, 1 mm thick laminate, with a $[\pm 45]_S$ layup, and (b) 120 mm wide, 2.1 mm thick laminate, with a $[(\pm 45)_2]_S$ layup.

4 EXPERIMENTS

4.1 Preliminary Investigation

To demonstrate the effect of the anticlastic behaviour on the bending stiffness of a composite laminate, two dual-matrix strips of different widths (10 mm and 40 mm) are cantilevered, and the deflections compared (see Figure 4(a)). Euler-Bernoulli beam theory suggests that the tip deflections should be the same for both laminates, since the ratios of the applied load (the laminate's own weight) to the second moment of area are equal, but in this case the deflections differ significantly. A third strip is cut with a width of 20 mm, and a slit is made along the middle of the flexible-matrix region (see Figure 4(b)) to ensure that the width of each half of the flexible region is 10 mm for a fair comparison. In this case, the laminates exhibit the same deflection, confirming that the effective bending stiffness of the flexible region is highly dependent on its width, and hence the anticlastic deflection. Figure 4(c) clearly shows the anticlastic effect occurring in the laminate for a large curvature. A simple FE simulation is conducted to characterize this phenomenon. The anticlastic deflections are compared with the analytical prediction at increasing distances from the fixed edge; the distance at which these equate is the point at which the flexible region is unaffected by the dual-matrix interaction. Interestingly, it is found that the distance is independent of curvature, and for a section that has a length at least 2.5 times the width, the anticlastic effect is unconstrained at the midpoint of the section.

(a)

(b)

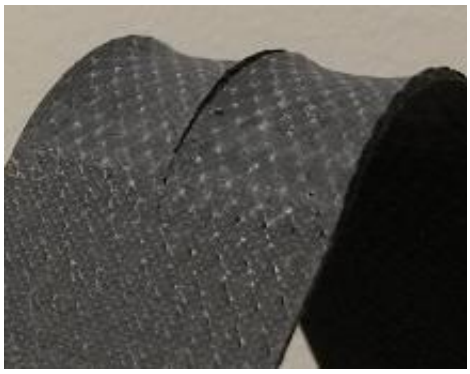

(c)

Figure 4. Bending stiffness comparison for (a) narrow and wide dual-matrix laminates, and (b) narrow laminate and wide laminate with a lengthwise slit in the elastomer region. (c) The anticlastic effect in a dual-matrix laminate.

4.2 Experimental Setup

Use of a typical MTS setup with a 100 kN load cell is impractical in this work, since it has a resolution of 10 N, which is far too large for the expected loads. An improvised setup is used (Figure 5) using the same bending rig. A camera is used to capture the anticlastic curvature of the test sample and a laser distance sensor, which measures the value of *H*, is used to determine the longitudinal radius of curvature induced by adding weight to each end of the test sample. The effective moment applied to the laminate is

$$M_{applied} = Fd + \frac{q}{2}\left(d^2 - \frac{W^2}{4}\right). \tag{7}$$

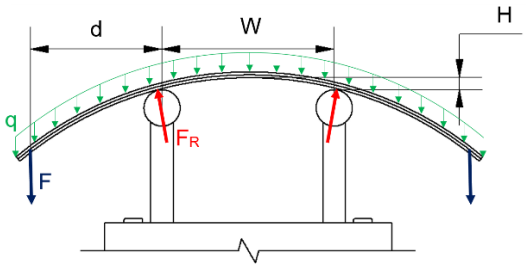

Figure 5. Four-point bending test setup and applied moment

4.3 Results

Due to the high compliance of the elastomeric laminate, only laminates 2 mm thick or greater can be used for the four-point bending test. Thinner laminates do not have sufficient bending stiffness to support their own weight, let alone provide accurate experimental data. Thus, the available experimental data set for this analysis is limited.

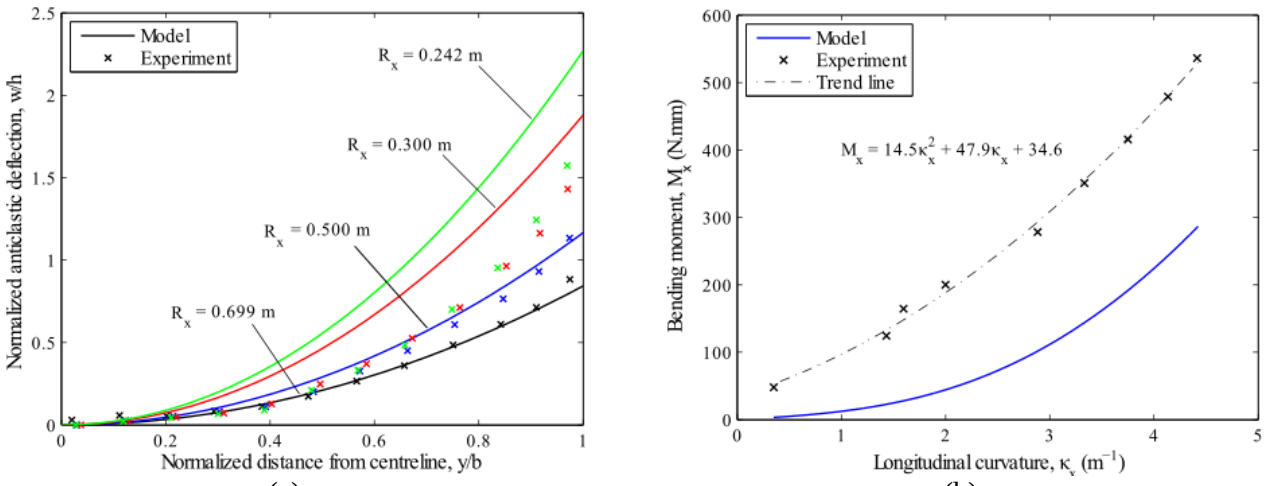

(a) (b)

Figure 6. Comparison between the analytical model and experimental data of a 100 mm wide $[(\pm 45F)_8]$ laminate for (a) anticlastic curvature, and (b) bending moment.

4.3.1 Anticlastic Bending

The coordinates of the laminate's top surface are extracted and normalized with respect to the laminate thickness and width. The theory demonstrates good correlation for narrow laminates, under-predicting the anticlastic edge deflections by less than 10% for larger curvatures. Figure 6 presents the theoretical and experimental results for a wider laminate. Figure 6(a) shows that the theoretical model exhibits good correlation only for small curvatures. As the curvature increases, the experimental results display an earlier transition to wide beam theory than predicted, which is evident from flattening close to the centre of the laminate.

4.3.2 Bending Moment

The bending moment predictions of the analytical model have been shown to correlate well with the finite element results. To validate these results the applied bending moment applied is plotted for increasing curvature, and compared with the analytical model. For both narrow and wide laminates, the model underestimates the bending stiffness of the samples. The reasons for this are discussed in the next section on CLT limitations. Thus, the analytical model is not suitable for predicting the bending stiffness of woven-fabric laminates. Nonetheless, the experiments confirm an increase in bending stiffness for increasing curvature. The results in Figure 6(b) for a wide laminate show a better correlation (in terms of curve gradient) compared to narrow laminates, which predict a nearly linear relationship for these relatively low curvatures. The neutral axis discrepancy between the FE and analytical models may explain the larger bending stiffness seen in the experimental results, if this shift is truly indicative of reality. However, there is insufficient evidence to conclude that this neutral axis shift occurs, since it is difficult to quantify in experiments.

4.3.3 Classical Lamination Theory Limitations

Despite CLT providing sufficiently accurate predictions for the behaviour of laminates with unidirectional plies, it does not accurately model the laminae interactions for such laminates, let alone woven laminates. CLT does not account for interlaminar shear effects, which are particularly influential in the bending behaviour of [±45] laminates. Since CLT is used in both the analytical model and FEA, it makes sense that these sets of data would correlate better than the experiments. The error can be attributed to the lack of accuracy for woven laminates. This can be best explained by considering the shear behaviour of the two [±45] laminates under an applied bending moment. Assuming no interlaminar effects, the fibres in unidirectional laminae are free to rotate due to

shear. Fibres in woven laminae, on the other hand, are constrained by the perpendicular interwoven fibres. The fibres in the +45 direction can no longer rotate freely since they are being constrained by the -45 fibres, and vice versa. Thus, the lamina will have greater stiffness than predicted. Reintroducing interlaminar effects, the stiffness is further increased due to the lamina rotation being additionally constrained. CLT accounts for neither, so the greater stiffness exhibited in the experiments is expected.

5 CONCLUSIONS

The material properties of a fibre composite with a polyurethane-based elastomeric matrix were first characterized experimentally for different layups, showing a uniaxial tensile stiffness of three orders of magnitude lower than that of carbon-fibre/epoxy. The elastic modulus obtained from the experimental testing was larger than those predicted by CLT due to the theory neglecting interlamina effects prominent in woven composites. The bending stiffness is non-linear, due to anticlastic effects resulting from the laminate undergoing bending deformation. A simple experiment showed that there is an induced stiffness in a dual matrix laminate when the anticlastic curvature is constrained. Using an anticlastic deflection model derived by Hyer and Bhavani, the anticlastic curvature of composites under pure bending has been modelled and verified with Abaqus FEA. The change in cross-section shape resulted in an increased second moment of area, and hence bending stiffness. The analysis showed that the increase was greatest for laminates with large width and small thickness.

Unlike the FEA, the experimental results displayed a large discrepancy, with the analytical model under-predicting the bending stiffness. However, the analytical predictions for the anticlastic deflection of the cross-section correlated well with the experimental results. Wider laminates under large curvatures showed the greatest discrepancy. The reason for these discrepancies was narrowed down to the composite layup. The analytical model and FE model specify a layup of unidirectional plies, whereas woven fabric was used in the experiments. The woven-fabric composites have increased shear stiffness, due to the woven laminae shear properties differing from that of unidirectional laminae

6 REFERENCES

[1] D. Platt, and C. A. Steeves, Tailoring the bending stiffness of elastomeric dual-matrix composites. Master's thesis, University of Toronto, 2016.

[2] C. Thill, J. Etches, I. Bond, K. Potter, and P. M. Weaver. Morphing skins. *Aeronautical Journal*, 112(3216):117-139, 2008.

[3] G. Murray, F. Gandhi, and C. Bakis. Flexible matrix composite skins for one-dimensional wing morphing. *Journal of Intelligent Material Systems and Structures*, 21:1771-1781, 2010.

[4] I. M. Jimenez. High-strain composites and dual-matrix composite structures. PhD thesis, California Institute of Technology, 2014.

[5] D. G. Ashwell. The anticlastic curvature of rectangular beams and plates. *J. Royal Aeronaut. Soc.*, 54, 1950.

[6] R. J. Pomeroy. The effect of anticlastic bending on the curvature of beams. *International Journal of Solids and Structures*, 6(2):277-285, 1970.

[7] J. F. Wang, R. H. Wagoner, D. K. Matlock, and F. Barlat. Anticlastic curvature in draw-bend springback. *International Journal of Solids and Structures*, 42(5-6):1287-1307, 2005.

[8] Y. C. Pao. Simple bending analysis of laminated plates by large-deflection theory. *Journal of Composite Materials*, 4(3):380-389, 1970.

[9] M. W. Hyer, and P. C. Bhavani. Suppression of anticlastic curvature in isotropic and composite plates. *International Journal of Solids and Structures*, 20(6):553-570, 1984.

[10] H. Ahmadi, C. A. Steeves, and C. Daraio. Mechanical characterization of elastic laminates for dual-matrix composites. Master's thesis, Swiss Federal Institute of Technology (ETH Zurich), 2016

[11] I. S. Raju and J. T. Wang. Classical laminate theory models for woven fabric composites. *Journal of Composites Technology & Research*, 16(4):289-303, 1994.